Letter

Connections between spin-orbit torques and unidirectional magnetoresistance in ferromagnetic-metal–heavy-metal heterostructures

L. Chen,[1,2] K. Zollner,[3] S. Parzefall,[2] J. Schmitt,[2] M. Kronseder,[2] J. Fabian,[3] D. Weiss,[2] and C. H. Back[1]

[1]*Department of Physics, Technical University of Munich, Garching b. Munich, Germany*

[2]*Institute of Experimental and Applied Physics, University of Regensburg, Regensburg, Germany*

[3]*Institute of Theoretical Physics, University of Regensburg, Regensburg, Germany*

(Received 7 April 2021; revised 8 July 2021; accepted 7 January 2022; published 18 January 2022)

We investigate the connections between current-induced spin-orbit torques and unidirectional magnetoresistance (UMR) by performing second harmonic longitudinal resistance measurements on Co/Pt bilayer with magnetic-field $\mu_0 H$ up to 10 T and temperature T down to 2 K. The fieldlike torque h_{FL} changes sign with varying Co thickness t_{Co}, which indicates that competing mechanisms, i.e., the spin Hall effect (SHE) and the inverse spin galvanic effect (iSGE), are responsible for the generation of h_{FL}. The sign of h_{FL} coincides with the sign of UMR induced by spin-dependent scattering. However, the dampinglike torque h_{DL} is proportional to the inverse Co thickness, with no sign reversal for all measured temperatures and t_{Co}, indicating that h_{DL} originates solely from the SHE. The generation of h_{DL} via iSGE can be further excluded because of the observation of an H-linear dependence of UMR, which, in turn, indicates the negligible exchange coupling between spin accumulation and ferromagnetic metal.

DOI: 10.1103/PhysRevB.105.L020406

Since the discovery of current-induced magnetization switching in ferromagnetic metal (FM, e.g., Co)/heavy metal (HM, e.g., Pt) heterostructures, two main spin-orbit related mechanisms have been proposed as the microscopic origin of spin-orbit torques (SOTs) [1,2]. One is the spin Hall effect (SHE) due to the spin-orbit interaction (SOI) in the bulk of HM; the other is the inverse spin galvanic effect (iSGE) due to the SOI at the FM/HM interface (in literature, the iSGE-SOTs have also been alternatively named as Rashba-SOTs) [3]. Both effects are expected to generate fieldlike and dampinglike SOTs, which are quantified by the corresponding fieldlike h_{FL} and dampinglike h_{DL} effective magnetic fields.

The dampinglike torque can counteract the Gilbert damping [4], i.e., the relaxation of the magnetization towards its equilibrium position, and is the key parameter for various spin-orbit related phenomena [5–8]. For SHE, a spin current along the z direction with spin orientation along the y direction traverses the FM/HM interface, and subsequently gets absorbed by the FM [Fig. 1(a)]. Thus, h_{DL} originates from the spin transfer torque mechanism similar to that in magnetic trilayer structures [9]. In contrast, for iSGE, h_{DL} is expected to appear due to the combined effects of interfacial current-induced spin accumulation and the exchange coupling between the spin accumulation and FM [3,10–13], which is schematically shown in Fig. 1(b). The minimal Hamiltonian $\mathcal{H}$ describing the iSGE is [3]

$$\mathcal{H} = \frac{\hbar^2 k^2}{2m^*} + \lambda(\mathbf{k}\times\boldsymbol{\sigma})\cdot\mathbf{z} - J_{\mathrm{ex}}\mathbf{m}\cdot\boldsymbol{\sigma}. \quad (1)$$

Here, $\hbar$ is the reduced Planck constant, $\mathbf{k}$ is the wave vector, m^* is the effective mass, λ is the Bychkov-Rashba SOI at the FM/HM interface, $\boldsymbol{\sigma}$ is the Pauli spin matrix, $\mathbf{m}$ is the unit magnetization, and J_{ex} is the exchange interaction between FM (in our case Co) and the electrons hosting the Bychkov-Rashba SOI. It should be noted that to generate a sizeable h_{DL} via iSGE, $J_{\mathrm{ex}} \gg \lambda k$ should be satisfied [3,10]. The existence of h_{DL} due to the iSGE has been shown and quantified in single crystalline ferromagnets with reduced symmetry, e.g., (Ga,Mn)As [10] and Fe/GaAs [13]. For bilayers, however, the situation is more complicated. Although previous theories based on Boltzmann equation and drift-diffusion analysis [14] predict that iSGE results in $h_{\mathrm{FL}} > h_{\mathrm{DL}}$, for SHE a larger h_{DL} is expected, and there is no simple way to disentangle which effect dominates the contribution to SOTs [3].

On the other hand, the unidirectional magnetoresistance (UMR) has also been observed in FM/HM bilayers [15,16]. Being different from twofold magnetoresistance effects like the anisotropic magnetoresistance (AMR) and the spin Hall magnetoresistance [17], which are even under reversal of either charge current or magnetization, the UMR is an odd effect with onefold symmetry. Early experiments [15,16] and theory [18] propose that interfacial spin-dependent scattering between the spin accumulation induced by SHE and magnetization, in analogy to the current-in-plane giant magnetoresistance (GMR) effect, is the major origin of UMR, and the magnitude of UMR is proportional to h_{DL} [19]. Later studies show that, besides interfacial spin-dependent scattering, bulk spin-dependent scattering [20] and electron-magnon scattering [20,21] also contribute to UMR. However, the studies of SOTs and UMR have been mostly performed independently so far. A proper correlation between these two important current-induced phenomena is yet to be established [19].

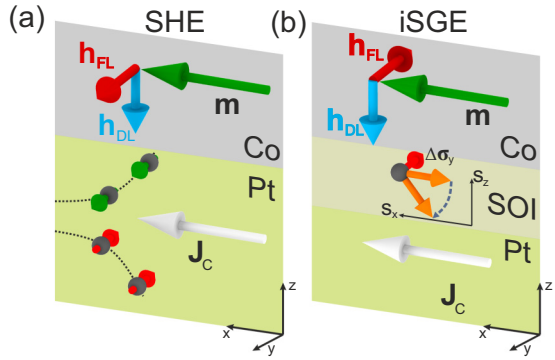

FIG. 1. Schematic of (a) SHE and (b) iSGE in real space. For SHE in (a), the SOI in Pt splits the spin-up and spin-down electrons carried by J_C. The spins along $+y$ direction, corresponding to a positive spin Hall angle, produce h_{FL} as well as h_{DL}. For iSGE in (b), a spin (orange arrow) at the interface with Bychkov-Rashba SOI is exchange coupled to the Co magnetization **m**. With current J_C, an additional spin accumulation $\Delta\boldsymbol{\sigma}_y$ along the $-y$ direction (red arrow), corresponding to a positive λ, is generated due to Bychkov-Rashba SOI. $\Delta\boldsymbol{\sigma}_y$ produces h_{FL} acting on Co. The combined action of exchange coupling and $\Delta\boldsymbol{\sigma}_y$ results in a nonzero tilt of the spin along the $-z$ direction (blue dashed arrow). In this case, an out-of-plane spin component i.e., h_{DL}, is generated.

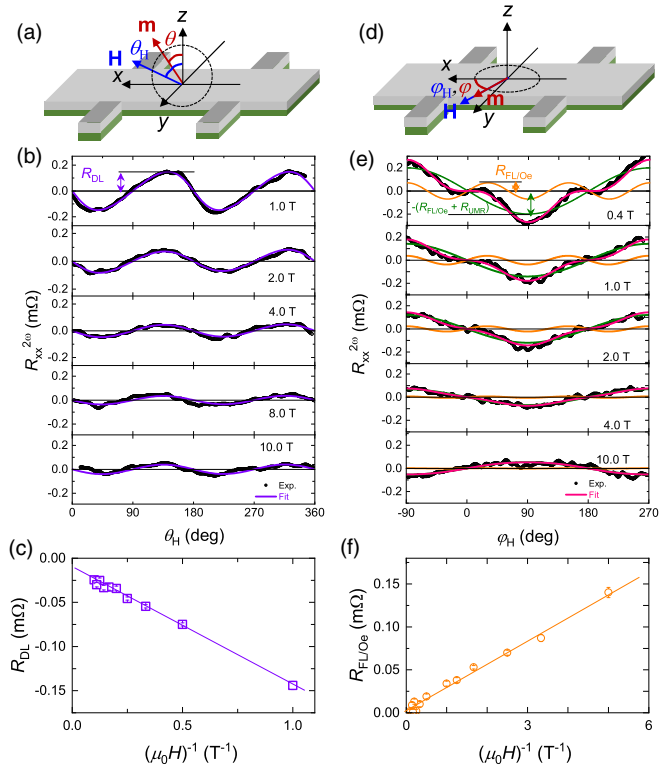

FIG. 2. (a) Illustration of the setup for rotating H and thus **m** in $x-z$ plane to measure h_{DL}. θ_H (θ) is the out-of-plane angle for H (**m**). (b) θ_H dependence of $R_{xx}^{2\omega}$ measured at $T = 200\,K$ and different magnetic fields for Co(1 nm)/Pt (4 nm). The points are experimental data, and solid lines are fits using Eq. (2) and R_{DL} is obtained. (c) $(\mu_0 H)^{-1}$ dependence of R_{DL}. The solid line is a linear fit; from the slope h_{DL} is determined. (d) Illustration of the setup to rotate H and **m** in $x-y$ plane to measure h_{FL} and UMR. φ_H (φ) is the in-plane angle for H (**m**). (e) φ_H dependence of $R_{xx}^{2\omega}$ measured at $T = 200\,K$ and different magnetic fields for Co(1 nm)/Pt (4 nm). Open points are experimental data, and solid lines are fits using Eq. (3) and $R_{FL/Oe}$ is obtained. (f) $(\mu_0 H)^{-1}$ dependence of $R_{FL/Oe}$. The solid line is a linear fit; from the slope h_{FL} is determined.

In this Letter, we report on second harmonic longitudinal resistance $R_{xx}^{2\omega}$ measurements [22] on Co/Pt samples for magnetic fields $\mu_0 H$ up to 10 T and temperature T down to 2 K; we simultaneously probe the SOTs and UMR. By varying the Co thickness t_{Co}, we find that h_{FL} changes sign when increasing t_{Co}. This indicates that both SHE and iSGE contribute to h_{FL} and that they add destructively. We find that h_{DL} is proportional to the inverse Co thickness, i.e., $h_{DL} \sim {t_{Co}}^{-1}$ without sign reversal in the examined T and t_{Co} range, suggesting that h_{DL} originates solely from the SHE. The sign of the UMR induced by spin-dependent scattering coincides with the sign of h_{FL}, showing cross matched results between UMR and SOTs. Moreover, UMR scales linearly with the magnetic field and does not saturate at higher magnetic fields, which can only be explained by assuming that the exchange coupling between the spin accumulation and FM is negligibly small, and thus the generation of h_{DL} via iSGE can be neglected.

To quantify SOTs and UMR, magneto-transport measurements are mainly carried out in two magnetic-field rotation schemes as shown in Figs. 2(a) and 2(d), i.e., in-plane to out-of-plane $x-z$ rotation to quantify h_{DL} and in-plane $x-y$ rotation to quantify h_{FL} as well as UMR [23]. Figure 2(b) presents out-of-plane magnetic-field angle θ_H dependence of $R_{xx}^{2\omega}$ for $t_{Co} = 1$ nm, measured from $\mu_0 H = 1$ to 10 T and $T = 200\,K$. The amplitude the signal decreases monotonically as H increases. h_{DL} can be quantified using [23]

$$R_{xx}^{2\omega} = -\frac{\Delta R_{AMR}}{2}\frac{h_{DL}}{H_K\cos 2\theta + H\cos(\theta_H - \theta)}\sin 2\theta. \quad (2)$$

Here ΔR_{AMR} is the AMR of Co, θ the out-of-plane angle for the magnetization. For $|H_K| \ll H$, Eq. (2) can be simplified to [23] $R_{xx}^{2\omega} = R_{DL}\sin 2\theta \approx -\frac{\Delta R_{AMR}}{2}\frac{h_{DL}}{H}\sin 2\theta$, and R_{DL} is the resistance induced by h_{DL}, which is obtained by fitting the $R_{xx}^{2\omega}$ traces. By plotting R_{DL} as a function of the inverse magnetic field $(\mu_0 H)^{-1}$, a linear relation with slope k_{DL} is obtained [Fig. 2(c)]. h_{DL} can be determined by $h_{DL} = -2k_{DL}/\Delta R_{AMR}$, where ΔR_{AMR} is obtained from the θ_H dependence of the first harmonic resistance in the same rotation plane [23].

Figure 2(e) shows the in-plane magnetic-field angle φ_H dependence of $R_{xx}^{2\omega}$ for the same device measured at different magnetic fields and $T = 200\,K$. For rotation in the $x-y$ plane $R_{xx}^{2\omega}$ can be expressed as [23]

$$\begin{aligned} R_{xx}^{2\omega} &= R_{FL/Oe}(\sin 3\varphi + \sin\varphi) + R_{UMR}\sin\varphi \\ &= R_{FL/Oe}\sin 3\varphi + (R_{FL/Oe} + R_{UMR})\sin\varphi \\ &= -\frac{\Delta R_{AMR}}{4}\frac{h_{FL} + h_{Oe}}{H}\sin 3\varphi + R_{UMR+FL/Oe}\sin\varphi, \end{aligned} \quad (3)$$

where $R_{FL/Oe}$ (being a function of $\sin 3\varphi$ and $\sin\varphi$) is the resistance induced by h_{FL} as well as in-plane Oersted field h_{Oe}. h_{Oe} is generated by current j_{Pt} flowing in Pt and can be calculated by $h_{Oe} = j_{Pt}t_{Pt}/2$, which is valid for $t_{Co} < 5$ nm. R_{UMR} is the magnitude of the UMR, the $\sin\varphi$ component $R_{UMR+FL/Oe}$

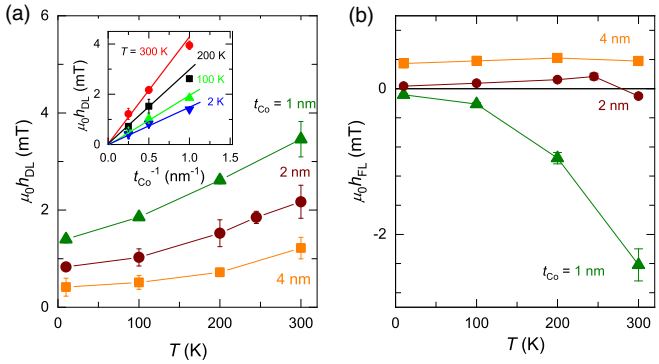

FIG. 3. (a) T dependence of h_{DL} at $j_{Pt} = 10^{11}$ A m^{-2}. The inset shows the linear dependence of h_{DL} on ${t_{Co}}^{-1}$ for each T. (b) T dependence of h_{FL} at $j_{Pt} = 10^{11}$ A m^{-2}. For some points in (a) and (b), the error bars are smaller than the symbol size.

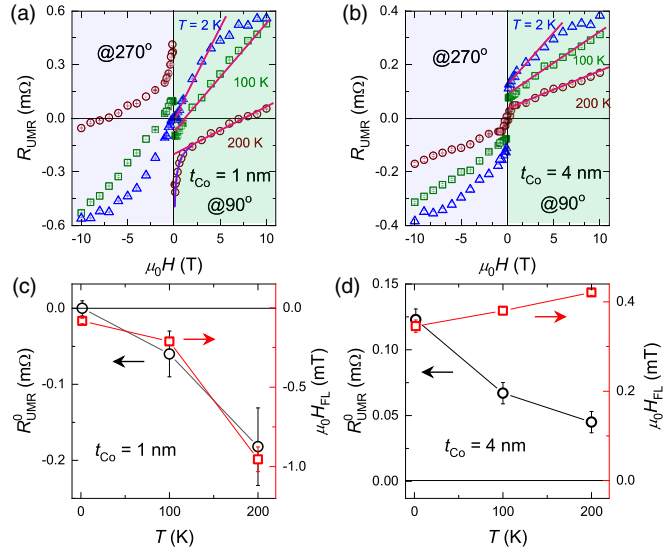

FIG. 4. $\mu_0 H$ dependence of R_{UMR} measured at different temperatures for $t_{Co} = 1$ nm (a) and $t_{Co} = 4$ nm (b). The pink solid lines are linear fits from which the spin-dependent R^0_{UMR} and the slope k_{UMR} are obtained. Note that due to nonlinearity of data at 2 K, data only between 1 and 5 T are fitted for both samples. The purple solid line of (a) is fitted by $R_{UMR} = R^0_{UMR} + b(\mu_0 H)^{-p}$, where b and p are coefficients describing the power-law decay of R_{UMR}. T dependence of R^0_{UMR} and h_{FL} for $t_{Co} = 1$ nm (c) and $t_{Co} = 4$ nm (d).

contains both $R_{FL/Oe}$ and R_{UMR}, i.e., $R_{UMR+FL/Oe} = R_{FL/Oe} + R_{UMR}$, and φ is the in-plane magnetization angle which satisfies $\varphi = \varphi_H$ because of the negligible in-plane uniaxial magnetic anisotropy field H_U [23]. For lower H, the $R^{2\omega}_{xx}$ trace can be decomposed into a sin3φ and a sinφ component, whose magnitudes are, respectively, related to $R_{FL/Oe}$ and $R_{UMR+FL/Oe}$. Similar to R_{DL}, $R_{FL/Oe}$ decreases as H increases and shows a linear dependence on H^{-1} [Fig. 2(f)]; h_{FL} can be obtained from $h_{FL} = -4k_{FL/Oe}/\Delta R_{AMR} + h_{Oe}$, where $k_{FL/Oe}$ is the slope of the linear fit. R_{UMR} can be obtained by $R_{UMR} = R_{UMR+FL/Oe} - R_{FL/Oe}$. Compared to $R_{FL/Oe}$, R_{UMR} evolves quite differently with H: R_{UMR} gradually decreases with increasing H from 0.4 to 4 T and even reverses its sign at 10 T. We note that the observed H dependence of R_{UMR} differs from previous reports [15] measured below 2 T, which will be discussed in detail below.

As shown in Fig. 2(c), the linear fit of $R_{DL} - H^{-1}$ almost goes through the origin with a negligible intercept. This indicates that magnetothermoelectric effects (specifically, the anisotropic magnetothermopower effect for the $x - z$ plane rotation, which has the same angular dependence as R_{DL} and gives rise to an H-independent $R^{2\omega}_{xx}$ signal due to a potential temperature gradient along the z direction) are absent for the Co/Pt devices [23]. We also show that the anomalous Nernst effect and the spin Seebeck effect can be excluded [23].

We repeat the same measurements as the ones shown in Fig. 2 for different Co thickness and temperatures. The T dependence of h_{DL} is summarized in Fig. 3(a). h_{DL} monotonically decreases as T decreases for all the samples which is due to a decrease of the bulk spin Hall angle of Pt [24] as well as an increase of the saturation magnetization of Co, and similar T and t_{FM} trends have been reported previously [25,26]. The inset shows that h_{DL} is a linear function of ${t_{Co}}^{-1}$, indicating that h_{DL} originates dominantly from the bulk SHE [Fig. 6(a) of Haney *et al.* [27]]. As shown in Fig. 3(b), h_{FL} shows a more complicated behavior and does not correlate with h_{DL} [28]. For $t_{Co} = 1$ nm, h_{FL} is negative and decreases rapidly with decreasing T, being consistent with previous studies [26,29–31]; in contrast, h_{FL} is positive for $t_{Co} = 4$ nm and decreases slowly as T decreases. This is a sign reversal of h_F induced by t_{Co} [32]. For $t_{Co} = 2$ nm, h_{FL} even changes sign from negative to positive around 250 K and decreases further with decreasing T. This has also been observed in a Pt(4 nm)/CoFe(0.6 nm) bilayer [29]. The sign reversal of h_{FL} with t_{Co} and T indicates that competing effects contribute to h_{FL}: one due to the bulk SHE generating h^{SHE}_{FL} and another due to the interfacial Bychkov-Rashba SOI [33] generating h^{iSGE}_{FL}. Based on these experimental facts, we deduce that h^{SHE}_{FL} and h^{iSGE}_{FL} add destructively, as schematically shown in Fig. 1.

The above results indicate that h_{DL} hardly originates from iSGE via the Bychkov-Rashba SOI. If iSGE would dominantly contribute to h_{DL}, one would also expect a sign reversal of h_{DL}, but this is not observed in the experiments. Here we exclude the generation of h_{DL} via iSGE by analyzing the H dependence of UMR. Figure 4(a) shows the H dependence of R_{UMR} for $t_{Co} = 1$ nm, which is extracted by fitting the traces in Fig. 2(e). At $T = 200\,K$, R_{UMR} decays following a power law as $\mu_0 H$ increases from 0 to 1 T, and this decay vanishes at lower temperatures. According to previous studies [20,21], this is due to the presence of electron-magnon scattering, which can be significantly suppressed at lower T where the density of magnons is reduced. Interestingly, for $\mu_0 H > 1T$, R_{UMR} shows a linear dependence on H and does not saturate even for magnetic field up to 10 T, which is observed for all samples [Figs. 4(a) and 4(b)]. Note that the magnetization is fully saturated by H as evidenced by AHE measurements [23]. We also show that the ordinary Nernst effect [34] can be excluded when considering the H-linear R_{UMR} [23]. At a temperature of 2 K, however, R_{UMR} becomes nonlinear for $\mu_0 H > 5\,T$. We also tried to measure R_{UMR} on reference devices fabricated from pure Co and Co/Cu bilayers. However, no characteristic R_{UMR} signals occurred using the same cur-

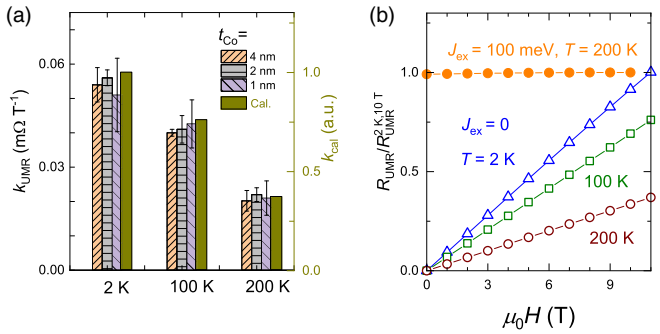

FIG. 5. (a) T dependence of k_{UMR} summarized for all samples; the calculated slope k_{cal} agrees with the experiment. (b) Theoretical calculations of $\mu_0 H$ dependence of R_{UMR} normalized by R_{UMR} at $T = 2\,K$ and $\mu_0 H = 10\,T$, $R_{\mathrm{UMR}}/R^{2\,\mathrm{K},10\,T}_{\mathrm{UMR}}$. The calculation without J_{ex} shows that the slope increases as T decreases (open symbols), which well reproduces the experimental results. In contrast, when taking J_{ex} ($J_{\mathrm{ex}} = 100\,\mathrm{meV} \gg \lambda k$) into account, R_{UMR} becomes almost independent of H (solid symbols), being inconsistent with experimental results.

rent excitation and magnetic field as for Co/Pt, indicating that R_{UMR} indeed originates from the SOI at the Co/Pt interface [23]. As shown by the solid lines in Figs. 4(a) and 4(b), the H-linear R_{UMR} is fitted by $R_{\mathrm{UMR}} = R^0_{\mathrm{UMR}} + k_{\mathrm{UMR}}\mu_0 H$, where R^0_{UMR} is the zero-field intercept which is independent of H, and k_{UMR} is the slope; their dependences on T and t_{Co} will be discussed below.

As suggested by previous experiments [15,16] and theory [18], the H-independent R^0_{UMR} can be ascribed to the combined effects of both interface and bulk spin-dependent scattering, similar to the effects occurring in GMR devices [35,36]. Figures 4(c) and 4(d) summarize the T dependence of R^0_{UMR} for $t_{\mathrm{Co}} = 1$ nm and 4 nm, respectively. R^0_{UMR} is negative for $t_{\mathrm{Co}} = 1$ nm, but changes sign for $t_{\mathrm{Co}} = 4$ nm. The t_{Co}-driven sign reversal of R^0_{UMR} coincides with the sign reversal of h_{FL} as shown in Fig. 3(b), which suggests that the net interfacial spin accumulation, originating from both SHE and iSGE and quantified by h_{FL}, determines the sign of R^0_{UMR}. Since both SHE and iSGE contribute to R^0_{UMR}, we refrain from calling it unidirectional spin Hall magnetoresistance as originally proposed [15], but rather call it UMR. Besides the sign reversal, the variation of R^0_{UMR} with temperature for these two samples also differs: for $t_{\mathrm{Co}} = 1$ nm, R^0_{UMR} decreases rapidly as T decreases; this trend is consistent with the T dependence of h_{FL} as shown in Fig. 4(c). In contrast, for $t_{\mathrm{Co}} = 4$ nm, shown in Fig. 4(d), R^0_{UMR} and h_{FL} show opposite T trends. These results indicate that, for thinner t_{Co} of 1 nm, the interfacial spin-dependent scattering, which is determined by the net interfacial spin accumulation (h_{FL}), dominates R^0_{UMR}. For thicker t_{Co}, the main contribution to R^0_{UMR} is bulk spin-dependent scattering, which leads to an enhanced R^0_{UMR} as T decreases due to an enhanced spin asymmetry [36].

The fact that R_{UMR} does not saturate at high magnetic fields, and scales with H but not the magnetization, indicates that, besides spin-dependent and electron-magnon scattering, there is a third mechanism contributing to R_{UMR}. The T dependence of the slope k_{UMR} is displayed in Fig. 5(a), which shows that k_{UMR} is independent of t_{Co} while k_{UMR} increases as T decreases. We note that a similar H-linear R_{UMR} has been reported in nonmagnetic materials with strong SOI, such as Rashba-type polar semiconductors BiTeBr [37], Ge (111) [38] and topological insulator Bi_2Se_3 [39]. There the origin of R_{UMR} has been ascribed to the interplay between magnetic field and the current-induced in-plane spin accumulation. To compare the magnitude of UMR for different material systems, we introduce $R_{\mathrm{UMR}} = \alpha j \mu_0 H$, where $\alpha (= k_{\mathrm{UMR}}/j)$ quantifies the H-linear R_{UMR} induced by j and H. The estimated α in Co/Pt is about $10^{-17}\,T^{-1}\,\mathrm{A}^{-1}\,m^2$. This value is several orders smaller than those in nonmagnetic materials [23], possibly due to a weaker SOI.

Since we observe a sizeable $h^{\mathrm{iSGE}}_{\mathrm{FL}}$, we propose that the H-linear R_{UMR} in Co/Pt results from the same mechanism as in nonmagnetic materials. On the other hand, $h^{\mathrm{SHE}}_{\mathrm{FL}}$ does not contribute to the H-linear R_{UMR} for two reasons: (i) for the SHE, the momentum and spin are not mutually locked; (ii) if both $h^{\mathrm{SHE}}_{\mathrm{FL}}$ and $h^{\mathrm{iSGE}}_{\mathrm{FL}}$ would contribute to the H-linear part, one would also expect that k_{UMR} changes sign like h_{FL} when changing t_{Co} (or, for $t_{\mathrm{Co}} = 2$ nm, a sign reversal by changing T). This, however, is not observed in the experiments. To describe the H-linear R_{UMR}, we include the Zeeman interaction in Eq. (1), i.e., $\mathcal{H} = \frac{\hbar^2 k^2}{2m^*} + \lambda(\mathbf{k} \times \boldsymbol{\sigma}) \cdot \mathbf{z} - (J_{\mathrm{ex}}\mathbf{m} + \mathrm{g}\mu_B\mu_0\mathbf{H}) \cdot \boldsymbol{\sigma}$, with g being the g factor and μ_{B} the Bohr magneton. Since R_{UMR} is expected to be proportional to the second order conductivity $\sigma^{(2)}_{xx}$ [21], we calculate $\sigma^{(2)}_{xx}$ based on nonlinear Boltzmann transport using a single-band constant relaxation time τ approximation [37], $\sigma^{(2)}_{xx} = -\frac{e^3\tau^2}{\hbar^2}\int \frac{\mathbf{dk}}{(2\pi)^2} v_x \frac{\partial^2 f}{\partial k_x^2}$. Here e is the electron charge, v_{x} is the electron group velocity along the current direction, and f is the Fermi distribution function [23]. Figure 5(b) presents the calculated H dependence of R_{UMR} using $m^* = m_0$ (m_0 is the free electron mass), $\lambda = 0.2\,\mathrm{eV\,\AA}$, $g = 2$. The calculation with $J_{\mathrm{ex}} = 0$ shows qualitative agreement with the experiments, i.e., R_{UMR} scales linearly with H and the slope increases as T decreases. In contrast, for a sizeable J_{ex} (e.g., $J_{\mathrm{ex}} = 100\,\mathrm{meV}$ and $J_{\mathrm{ex}} \gg \lambda k$, which satisfies the condition to generate h_{DL} via iSGE), the calculated R_{UMR} varies weakly with H, being inconsistent with the experimental results. Thus, these results indicate that J_{ex} is negligibly small in Co/Pt. Another alternative way to exclude J_{ex} is using an elegant model, which was developed by Guillet *et al.* [38], to interpret the UMR in Ge. Assuming that $h^{\mathrm{iSGE}}_{\mathrm{FL}} \ll H$, R_{UMR} can be written as $R_{\mathrm{UMR}} = A h^{\mathrm{iSGE}}_{\mathrm{FL}} H \sin\varphi_{\mathrm{H}}$, here A quantifies the magnitude of R_{UMR}. This model well describes dependence of R_{UMR} on φ_{H} and H in Ge. By applying it to Co/Pt and taking the exchange field as a pseudomagnetic field ($J_{\mathrm{ex}}/g\mu_{\mathrm{B}}$), the H-linear R_{UMR} in Co/Pt can be obtained as $R_{\mathrm{UMR}} = A h^{\mathrm{iSGE}}_{\mathrm{FL}}(J_{\mathrm{ex}}/g\mu_{\mathrm{B}} + \mu_0 H)\sin\varphi_{\mathrm{H}}$. Based on this equation, one can explain an H-linear R_{UMR} on the condition that $J_{\mathrm{ex}}/g\mu_B \ll \mu_0 H$, i.e., for negligible J_{ex} only. This indicates that the Rashba layer is not exactly located at the interface, but is "far" from the interface. Besides the location of the Rashba layer, future experimental and theoretical work are needed to unveil the following: (i) What are the electronic orbits (s, p, or d) contributing to the Rashba spin-orbit interaction? (ii) How large is the exchange interaction between Co and "Rashba electrons"? Thus, answering these questions in a proper way will definitely help us to gain a deeper

understanding of the mechanisms of SOTs in the Co/Pt system and in general.

In summary, we have performed second harmonic longitudinal resistance measurements on Co/Pt samples simultaneously probing SOTs and UMR. By varying t_{Co}, we find that h_{FL} changes sign upon increasing t_{Co} while $h_{DL} \sim {t_{Co}}^{-1}$. This suggests that h_{FL} originates from both iSGE and SHE but h_{DL} stems only from SHE. The generation of h_{DL} via iSGE is excluded since the exchange interaction between the local magnetization and the Bychkov-Rashba electrons is negligible, which is experimentally confirmed by the observation of an H-linear dependence of R_{UMR}. Our results clarify the origins of SOTs in metallic bilayer systems and resolve the long-time controversial views.

We would like to thank C. Gorini for useful discussions. This work is supported by the German Science Foundation (DFG) via SFB 1277.

[1] I. M. Miron, K. Garello, G. Gaudin, P. Zermatten, M. V. Costache, S. Auffret, S. Bandiera, B. Rodmacq, A. Schuhl, and P. Gambardella, Nature (London) **476**, 189 (2011).

[2] L. Q. Liu, O. J. Lee, T. J. Gudmundsen, D. C. Ralph, and R. A. Buhrman, Phys. Rev. Lett. **109**, 096602 (2012).

[3] A. Manchon, J. Železný, I. M. Miron, T. Jungwirth, J. Sinova, A. Thiaville, K. Garello, and P. Gambardella, Rev. Mod. Phys. **91**, 035004 (2019).

[4] K. Ando, S. Takahashi, K. Harii, K. Sasage, J. Ieda, S. Maekawa, and E. Saitoh, Phys. Rev. Lett. **101**, 036601 (2008).

[5] L. Q. Liu, C. F. Pai, Y. Li, H. W. Tseng, D. C. Ralph, and R. A. Buhrman, Science **336**, 555 (2012).

[6] M. M. Decker, M. S. Wörnle, A. Meisinger, M. Vogel, H. S. Körner, G. Y. Shi, C. Song, M. Kronseder, and C. H. Back, Phys. Rev. Lett. **118**, 257201 (2017).

[7] V. E. Demidov, S. Urazhdin, H. Ulrichs, V. Tiberkevich, A. Slavin, D. Baither, G. Schmitz, and S. O. Demokritov, Nat. Mater. **11**, 1028 (2012).

[8] S. Emori, U. Bauer, S. Ahn, E. Martinez, and G. S. D. Beach, Nat. Mater. **12**, 611 (2013).

[9] D. C. Ralph and M. D. Stiles, J. Magn. Magn. Mater. **320**, 1190 (2008).

[10] H. Kurebayashi, J. Sinova, D. Fang, A. C. Irvine, T. D. Skinner, J. Wunderlich, V. Novák, R. P. Campion, B. L. Gallagher, E. K. Vehstedt, L. P. Zârbo, K. Výborný, A. J. Ferguson, and T. Jungwirth, Nat. Nanotechnol. **9**, 211 (2014).

[11] H. Li, H. Gao, L. P. Zârbo, K. Výborný, X. Wang, I. Garate, F. Doğan, A. Čejchan, J. Sinova, T. Jungwirth, and A. Manchon, Phys. Rev. B **91**, 134402 (2015).

[12] A. Qaiumzadeh, R. A. Duine, and M. Titov, Phys. Rev. B **92**, 014402 (2015).

[13] L. Chen, M. Decker, M. Kronseder, R. Islinger, M. Gmitra, D. Schuh, D. Bougeard, J. Fabian, D. Weiss, and C. H. Back, Nat. Commun. **7**, 13802 (2016).

[14] V. P. Amin and M. D. Stiles, Phys. Rev. B **94**, 104420 (2016).

[15] C. O. Avci, K. Garello, A. Ghosh, M. Gabureac, S. F. Alvarado, and P. Gambardella, Nat. Phys. **11**, 570 (2015).

[16] K. Olejník, V. Novák, J. Wunderlich, and T. Jungwirth, Phys. Rev. B **91**, 180402(R) (2015).

[17] H. Nakayama, M. Althammer, Y. T. Chen, K. Uchida, Y. Kajiwara, D. Kikuchi, T. Ohtani, S. Geprägs, M. Opel, S. Takahashi, R. Gross, G. E. W. Bauer, S. T. B. Goennenwein, and E. Saitoh, Phys. Rev. Lett. **110**, 206601 (2013).

[18] S. S.-L. Zhang and G. Vignale, Phys. Rev. B **94**, 140411(R) (2016).

[19] C. O. Avci, K. Garello, J. Mendil, A. Ghosh, N. Blasakis, M. Gabureac, M. Trassin, M. Fiebig, and P. Gambardella, Appl. Phys. Lett. **107**, 192405 (2015).

[20] C. O. Avci, J. Mendil, G. S. D. Beach, and P. Gambardella, Phys. Rev. Lett. **121**, 087207 (2018).

[21] K. Yasuda, A. Tsukazaki, R. Yoshimi, K. S. Takahashi, M. Kawasaki, and Y. Tokura, Phys. Rev. Lett. **117**, 127202 (2016).

[22] B. Han, B. Wang, Z. Yan, T. Wang, D. Yang, X. Fan, Y. Wang, and J. Cao, Phys. Rev. Appl. **13**, 014065 (2020).

[23] See Supplemental Material at http://link.aps.org/supplemental/10.1103/PhysRevB.105.L020406 for sample and experimental details, the theory of 2ω magnetotransport method, the exclusion of thermoelectric effects, UMR measurements in $y-z$ plane scan, UMR measurements for control samples, and Boltzmann theory of the H-linear RUMR, where Refs. [40–45] are also included.

[24] M. Isasa, E. Villamor, L. E. Hueso, M. Gradhand, and F. Casanova, Phys. Rev. B **91**, 024402 (2015).

[25] C. F. Pai, Y. Ou, L. H. Vilela-Leão, D. C. Ralph, and R. A. Buhrman, Phys. Rev. B **92**, 064426 (2015).

[26] X. Fan, H. Celik, J. Wu, C. Ni, K. Lee, V. O. Lorenz, and J. Q. Xiao, Nat. Commun. **5**, 3042 (2014).

[27] P. M. Haney, H. W. Lee, K. J. Lee, A. Manchon, and M. D. Stiles, Phys. Rev. B **87**, 174411 (2013).

[28] C. O. Avci, G. S. D. Beach, and P. Gambardella, Phys. Rev. B **100**, 235454 (2019).

[29] X. Qiu, P. Deorani, K. Narayanapillai, K. Lee, Lee K, H. Lee, and H. Yang, Sci. Rep. **4**, 449 (2014).

[30] J. Kim, J. Sinha, S. Mitani, M. Hayashi, S. Takahashi, S. Maekawa, M. Yamanouchi, and H. Ohno, Phys. Rev. B **89**, 174424 (2014).

[31] Y. Ou, C. F. Pai, S. Shi, D. C. Ralph, and R. A. Buhrman, Phys. Rev. B **94**, 140414(R) (2016).

[32] T. D. Skinner, M. Wang, A. T. Hindmarch, A. W. Rushforth, A. C. Irvine, D. Heiss, H. Kurebayashi, and A. J. Ferguson, Appl. Phys. Lett. **104**, 062401 (2014). In this work, a sign reversal of $h_{FL/Oe}$ is observed when increasing t_{Co}. However, it is difficult to quantify the magnitude of the microwave current for STT-FMR measurements, and thus it is impossible to extract h_{FL} from the measured $h_{FL/Oe}$.

[33] H. Yang, O. Boulle, V. Cros, A. Fert, and M. Chshiev, Sci. Rep. **8**, 12356 (2018).

[34] N. Roschewsky, E. S. Walker, P. Gowtham, S. Muschinske, F. Hellman, S. R. Bank, and S. Salahuddin, Phys. Rev. B **99**, 195103 (2019).

[35] J. M. George, L. G. Pereira, A. Barthélémy, F. Petroff, L. Steren, J. L. Duvail,A. Fert, R. Loloee, P. Holody, and P. A. Schroeder, Phys. Rev. Lett. **72**, 408 (1994).

[36] C. Vouille, A. Barthélémy, F. E. Mpondo, A. Fert, P. A. Schroeder, S. Y. Hsu, A. Reilly, and R. Loloee, Phys. Rev. B **60**, 6710 (1999).

[37] T. Ideue, K. Hamamoto, S. Koshikawa, M. Ezawa, S. Shimizu, Y. Kaneko, Y. Tokura, N. Nagaosa, and Y. Iwasa, Nat. Phys. **13**, 578 (2017).

[38] T. Guillet, C. Zucchetti, Q. Barbedienne, A. Marty, G. Isella, L. Cagnon, C. Vergnaud, H. Jaffrès, N. Reyren, J. M. George, A. Fert, and M. Jamet, Phys. Rev. Lett. **124**, 027201 (2020).

[39] P. He, S. Zhang, D. Zhu, Y. Liu, Y. Wang, J. Yu, G. Vignale, and H. Yang, Nat. Phys. **14**, 495 (2018).

[40] Y. Du, S. Takahashi, and J. Nitta, Phys. Rev. B **103**, 094419 (2021).

[41] M. H. Nguyen, D. C. Ralph, and R. A. Buhrman, Phys. Rev. Lett. **116**, 126601 (2016).

[42] O. Stejskal, A. Thiaville, J. Hamrle, S. Fukami, and H. Ohno, Phys. Rev. B **101**, 235437 (2020).

[43] M. Hayashi, J. Kim, M. Yamanouchi, and H. Ohno, Phys. Rev. B **89**, 144425 (2014).

[44] K. Garello, I. M. Miron, C. O. Avci, F. Freimuth, Y. Mokrousov, S. Blügel, S. Auffret, O. Boulle, G. Gaudin, and P. Gambardella, Nat. Nanotechnol. **8**, 587 (2013).

[45] P. He, S. S.-L. Zhang, D. Zhu, S. Shi, O. G. Heinonen, G. Vignale, and H. Yang, Phys. Rev. Lett. **123**, 016801 (2019).